AFRL-RX-WP-TP-2011-4232

A MODEL FOR ESTIMATING NONLINEAR DEFORMATION AND DAMAGE IN CERAMIC MATRIX COMPOSITES (PREPRINT)

Unni Santhosh and Jalees Ahmad

Research Applications, Inc.

JULY 2011

AIR FORCE RESEARCH LABORATORY
MATERIALS AND MANUFACTURING DIRECTORATE
WRIGHT-PATTERSON AIR FORCE BASE, OH 45433-7750
AIR FORCE MATERIEL COMMAND
UNITED STATES AIR FORCE

REPORT DOCUMENTATION PAGE

Form Approved
OMB No. 0704-0188

1. REPORT DATE *(DD-MM-YY)*	2. REPORT TYPE	3. DATES COVERED *(From - To)*
July 2011	Journal Article Preprint	01 July 2011 – 01 July 2011

4. TITLE AND SUBTITLE
A MODEL FOR ESTIMATING NONLINEAR DEFORMATION AND DAMAGE IN CERAMIC MATRIX COMPOSITES (PREPRINT)

5a. CONTRACT NUMBER
In-house

5b. GRANT NUMBER

5c. PROGRAM ELEMENT NUMBER
62102F

6. AUTHOR(S)
Unni Santhosh and Jalees Ahmad

5d. PROJECT NUMBER
4347

5e. TASK NUMBER
20

5f. WORK UNIT NUMBER
LN101100

7. PERFORMING ORGANIZATION NAME(S) AND ADDRESS(ES)
Research Applications, Inc.
11772 Sorrento Valley Road, Suite 260
San Diego, CA 92121-1085

8. PERFORMING ORGANIZATION REPORT NUMBER

9. SPONSORING/MONITORING AGENCY NAME(S) AND ADDRESS(ES)
Air Force Research Laboratory
Materials and Manufacturing Directorate
Wright-Patterson Air Force Base, OH 45433-7750
Air Force Materiel Command
United States Air Force

10. SPONSORING/MONITORING AGENCY ACRONYM(S)
AFRL/RXLM

11. SPONSORING/MONITORING AGENCY REPORT NUMBER(S)
AFRL-RX-WP-TP-2011-4232

12. DISTRIBUTION/AVAILABILITY STATEMENT
Approved for public release; distribution unlimited.

13. SUPPLEMENTARY NOTES
PAO Case Number: 88ABW 2010-3935; Clearance Date: 21 Jul 2010. Document contains color.
Journal article submitted to the *Journal of Composite Materials*.

14. ABSTRACT
The present paper addresses estimation of global deformation of a continuous-fiber brittle matrix composite over a length much larger than the largest microstructural dimension of the composite, such as the fiber diameter and the fiber spacing. Initial microcracks and progressive microcracking of the matrix and interfaces under time-dependent load and temperature are considered. The model also includes consideration of inelastic deformation of one of the constituents. In this paper, the equations of the model are developed and applied to model the stress-strain behavior of several SiC/SiC CMCs and the creep behavior of an oxide/oxide CMC. Comparison with test data shows that the model is able to capture the wide range of deformation behavior seen in these CMCs.

15. SUBJECT TERMS
continuous-fiber brittle matrix composite, microcracks, progressive microcracking, SiC/SiC CMCs

16. SECURITY CLASSIFICATION OF:			17. LIMITATION OF ABSTRACT:	18. NUMBER OF PAGES	19a. NAME OF RESPONSIBLE PERSON (Monitor)
a. REPORT	b. ABSTRACT	c. THIS PAGE			Reji John
Unclassified	Unclassified	Unclassified	SAR	32	19b. TELEPHONE NUMBER *(Include Area Code)* N/A

A Model for Estimating Nonlinear Deformation and Damage in Ceramic Matrix Composites

Unni Santhosh and Jalees Ahmad
Research Applications, Inc., 11772 Sorrento Valley Rd, Suite 260, San Diego, CA 92121-1085, United States

Abstract

The present paper addresses estimation of global deformation of a continuous-fiber brittle matrix composite over a length much larger than the largest microstructural dimension of the composite, such as the fiber diameter and the fiber spacing. Initial microcracks and progressive microcracking of the matrix and interfaces under time-dependent load and temperature are considered. The model also includes consideration of inelastic deformation of one of the constituents. In this paper the equations of the model are developed and applied to model the stress-strain behavior of several SiC/SiC CMCs and the creep behavior of an oxide/oxide CMC. Comparison with test data shows that the model is able to capture the wide range of deformation behavior seen in these CMCs.

Introduction

A distinguishing characteristic of the class of ceramic-matrix composites is that the stress (σ) and time (t) dependent strain ($\varepsilon\{\sigma, t\}$), is partly due to micromechanical damage in the form of matrix cracks and/or interfacial separations and partly due to inelastic deformation of a constituent. Detailed observations on such composites have been presented by Karandikar and Chou [1], Zhu, et. al. [2] and others. Time dependence of damage and deformation mechanisms due to creep and due to chemical reaction of constituents with surrounding environment have been discussed by DiCarlo [3], Morscher [4], Eckel [5] and others. Based on observations reported in the literature, Figure 1 is a schematic representation of microscopic damage and deformation mechanisms and their manifestation on macroscopic strain, $\varepsilon\{\sigma, t\}$, of the composite.

Under monotonically increasing load over a short time, general tensile stress-strain behavior of the composite is shown in Figure 1(a). It shows an approximately linear portion (regions 1 and 2), followed by a gradually decreasing slope ($d\sigma/d\varepsilon$) in region 3, and subsequent stiffening in region 4. Relative size of each region varies with material system. For example, in some materials, composite rupture occurs without any perceptible stiffening. In others, presence of microcracks in as-fabricated condition can result in virtual absence of regions 1 and 2, resulting in a stress-strain curve that is nonlinear throughout.

The stress at the end of region 1 is the 'proportional limit', where a discernable deviation from the initial linear behavior occurs. Up to a certain stress, usually less than the proportional limit, the composite suffers no additional damage. However, pre-existing defects and damage (such as matrix porosity, interfacial disbonds and microcracks) may be present, affecting the initial slope as well as the proportional limit.

Transverse microcracks first appear, usually within the transverse tows in woven composites, at a stress less than the proportional limit [1], shown as start of region 2 in Figure 1(a). Some microcracks may be "gaps" among fibers within transverse tows due to insufficient matrix material penetration into the tows. Such gaps can open up under very low load. The onset of microcracking may also be influenced by composite processing induced residual stresses due to mismatch of coefficient of thermal expansion (CTE) among the constituents. Under increasing load microcracks enlarge, additional microcracks form, and splits (longitudinal cracks or interfacial disbonds) appear in region 2 as the applied stress approaches often a distinct knee in the stress-strain curve. Higher stress (region 3) causes accelerated microcracking accompanied by enlargement of splits. Some longitudinal fibers may fracture toward the end of region 3 as increasing matrix damage causes accelerated load transfer to the fibers. In region 4, applied load is carried largely by the longitudinal fibers, which eventually fracture, usually in rapid succession, resulting in composite rupture.

As shown in Figure 1(a), with insufficient time for significant time dependant deformations to have occurred, unloading from various stress levels and reloading is approximately linear, with little or no permanent deformation. However, hysteresis loops occur in some composites, especially at elevated temperatures.

Figure 1(b) depicts strain-time response of the composite under a constant applied load and at a sufficiently high temperature for constituent creep and/or chemical reaction of constituents with surrounding environment to be significant. The sequence of micromechanical damage progression with time is conjectured to be similar to that under increasing tensile load, but observations reported in the literature are less definitive because of difficulties associated with experiments at high temperatures. At constant applied load, strain increase can be due to creep of one or more constituents, interfacial sliding, additional microcracks and crack growth in the matrix, and discrete fiber fractures induced by reaction with environment. For example, in some composites, oxidation of the matrix can lower its strength, resulting in gradually increasing number of microcracks under constant applied load.

Depending on the composite, a portion of the time dependent strain may be permanent. Creep of one or more constituents, irreversible sliding at interfaces, and "wedging" of microcracks by reaction products are among plausible causes for permanent deformation.

There are several reported approaches in the literature for modeling micromechanical damage and deformation mechanisms in the types of composites presently considered. The model of Aveston, Cooper and Kelly [6] has served as the basis of a number of approaches, with significant improvements and generalizations by Marshall, Cox and Evans [7], Curtin [8] and others. A detailed mechanics analysis of matrix cracks by Budiansky, Hutchinson and Evans [9] and of fiber creep by Begley, Evans and McMeeking [10] have further enhanced the understanding of damage and deformation of brittle matrix composites. More recently, the stress-strain behavior of CMCs has been modeled using a phenomenological approach [11] and using continuum damage-based

approach [12-15]. None of these approaches however considers inelastic deformation of the constituents, and in most instances, the models require the testing of a range of different laminate configurations in order to obtain the inputs required for the application of the model.

The approach in the present work builds on several concepts and ideas found in references [6-10], and introduces extensions and enhancements aimed at improved modeling of deformation and damage mechanisms in CMCs relevant to current engineering applications. Special attention is given to developing models that include consideration of at least all the dominant damage and deformation mechanisms, while keeping the model reasonably simple, computationally efficient, and minimizing the number of laboratory tests needed to generate input for the model.

Model Derivation

To simplify presentation of the model, let us consider a two-phase composite, with fiber and matrix as the only constituent materials. In such a material the longitudinal and transverse stiffness of the composite can be approximated by the rule-of-mixtures (ROM) and the inverse ROM respectively [16]. Furthermore, let us prescribe the matrix material to be linear-elastic. Let us express the inelastic strain rate of the fiber material by the following three-dimensional *(k* and *l = 1,3)* rate form of the Prandtl-Reuss equations:

$$\dot{\varepsilon}^{i}_{kl(f)} = \lambda S_{kl(f)}, \tag{1}$$

where λ is a scalar function of state variables. If the fiber is in pure axial tension, with all other stress components being zero,

$$\dot{\varepsilon}^{i}_{f} = \frac{2}{3}\lambda\sigma_{f} \tag{2}$$

Both the matrix and the fiber materials are assumed homogeneous. It is implied that any porosity in the matrix is uniformly distributed and the largest pore size is small compared to the woven-architecture dimensions such as tow diameters and tow spacing. Therefore, porous matrix can be approximated as homogeneous, albeit with mechanical and thermal properties different than a fully dense matrix material. For example, the Young's Modulus of the matrix can be estimated as: $E_M = (1-p)E_{M(dense)}$, where p is the total volume of pores divided by the volume of the matrix in the composite. Similarly, other mechanical and thermal properties of a porous matrix can be estimated. Of course, more accurate models to account for porosity are possible. But, for the present, these simple estimates suffice.

Composite Without Damage

Let us first consider a strip of length *2L*, width W_U, and uniform thickness *d*, of a composite without damage, and having v_f volume of fibers per unit volume of the

composite (i.e., the average fiber volume fraction is v_f). The field quantities specific to the undamaged composite are identified with the subscript "*U*". The length is along one of the fiber directions. Each edge of the strip is displaced an amount (δ_U) by a force P_U acting normal to the cross-section $(W_U \cdot d)$. Thus, the average stress on the composite is $\sigma_U = P_U/(W \cdot d)$ and the total strain is $\varepsilon_U = \delta_U/L$. Each dimension of the composite strip is large compared to microstructural dimensions of the composite. In the case of a woven composite, microstructural dimensions include dimension of fiber-tow and the amplitude and wavelength characteristics of the weave.

If the composite is unidirectional, the applied stress σ_U is supported by the matrix and the fibers. In a woven composite with orthogonal tows, σ_U is shared by the longitudinal fibers, the matrix, and the transverse fibers. If the wave-length to amplitude ratio of the weave is large, such a woven composite can be viewed as a balanced cross-ply laminate, i.e. a $(0/90)_s$ laminate, with equal volume of fibers ($v_f/2$) in the load (0^o) direction and the transverse (90^o) direction. In that case, the woven composite can be approximated as a unidirectional composite having $v_f/2$ fiber volume fraction, and a matrix composed of the actual matrix material (*M*) and the transverse fibers. Let us denote this 'effective' matrix by *m*, and half the fiber volume fraction by V_f, such that, for a unidirectional composite, *m* is the same as *M* and $V_f = v_f$.

In woven composites, fiber-tows may contain matrix (*M*), voids, and individual fibers, with a different fiber volume fraction (v_{fw}) within the tows than the average volume fraction (v_f) in the composite. In that case, $v_f = v_w \cdot v_{fw}$, where v_w is the volume of tows per unit volume of the composite.

Assume that under time-dependent applied stress, $\sigma_U(t)$, the fibers *(f)* and the effective matrix *(m)* undergo the same total average strain rate ($\dot{\varepsilon}_U$), i.e.,

$$\dot{\varepsilon}_U = \dot{\varepsilon}_{Uf} = \dot{\varepsilon}_{Um} \tag{3}$$

At strain (ε_U) equal to zero, the fiber and the matrix may have initial (residual) stresses R_f and R_m, respectively, induced by the composite fabrication process. For example, the residual stresses can be due to unequal thermal contraction characteristic of the two materials during cool-down from some stress-free temperature (T_p) to a reference temperature (T_r). Simple estimates of such thermal residual stresses can be obtained using, for example, thermoelastic analysis results of Gatewood [17] for concentric cylinders of dissimilar materials.

The strain rate in the fiber consists of elastic, thermal and inelastic strain rates, i.e.,

$$\dot{\varepsilon}_U = D_t\left(\frac{\sigma_{Uf} - R_f}{E_f} + \alpha_f (T - T_r)\right) + \frac{2}{3}\lambda_{Uf}\sigma_{Uf} \quad , \tag{4}$$

where, D_t denotes derivative of the quantity within parenthesis with respect to time, and $T=T\{t\}$, $E_f=E_f\{T\}$ and $\alpha_f=\alpha_f\{T\}$ are the temperature, longitudinal fiber modulus and fiber CTE respectively.

Eq. (4) can be rearrange to give:

$$\dot{\sigma}_{Uf} = E_f\left[\dot{\varepsilon}_U - \sigma_{Uf} D_t\left(1/E_f\right) - D_t\left(\alpha_f\left(T-T_r\right) - \frac{R_f}{E_f}\right) - \frac{2}{3}\lambda_{Uf}\sigma_{Uf}\right] \tag{5}$$

The matrix being linear elastic,

$$\dot{\varepsilon}_U = D_t\left(\frac{\sigma_{Um} - R_m}{E_m} + \alpha_m(T - T_r)\right), \tag{6}$$

Here E_m and α_m are the Young's modulus and CTE of the effective matrix respectively. As mentioned earlier in a unidirectional composite system the effective matrix is the same as the actual matrix, but in a balanced cross-ply system the Young's modulus and CTE of the effective matrix have to be determined. Expressions for these quantities in terms of the longitudinal (E_f) and transverse (E_{fT}) modulus of the fiber, Poisson's ratio (υ_f) and CTE (α_f) of the fiber, the modulus (E_M), Poisson's ratio (υ_M) and CTE (α_M) of the actual matrix and the volume fraction of the fiber (v_f) are given in the appendix.

Note that with the assumptions already cited,

$$\sigma_U = V_f\sigma_{Uf} + V_m\sigma_{Um}, \tag{7}$$

$$E_U = V_f E_f + V_m E_m, \tag{8}$$

and, the matrix being linear elastic,

$$\sigma_{Um} = E_m(\varepsilon_U - \alpha_m(T - T_r)) + R_m. \tag{9}$$

Note that, depending on how the volume of voids in the matrix and the tows is accounted for, the volume fraction of the matrix (V_m) may not equal $(1\text{-}V_f)$, and that V_f and V_m can be functions of time and temperature.

Therefore,

$$\sigma_{Uf} = \frac{\sigma_U - V_m\left[E_m(\varepsilon_U - \alpha_m(T - T_r)) + R_m\right]}{V_f} \tag{10}$$

Substituting Eqs. (5) and (11) in Eq. (6), we get,

$$\dot{\varepsilon}_U = \left[\frac{\sigma_U - \left[E_m\left(\varepsilon_U - \alpha_m(T-T_r)\right) + R_m\right]V_m}{V_f}\right]\left[\frac{2}{3}C_f\lambda_{Uf} + C_T\right] + C_{fm} + C_m D_t\left(\frac{\sigma_U}{V_m E_m}\right) \qquad (11)$$

In the above equation,

$C_f = V_f E_f / E_U$,

$C_m = V_m E_m / E_U$,

$$C_{fm} = C_f D_t\left(\alpha_f(T-T_r) - \left(\frac{R_f}{E_f}\right)\right) + C_m D_t\left(\alpha_m(T-T_r) - \left(\frac{R_m}{E_m}\right)\right)$$

and

$$C_T = C_f D_t\left(\frac{1}{E_f}\right) - C_m D_t\left(\frac{V_f}{V_m E_m}\right)$$

Eq. (11), together with an appropriate initial condition, can be solved for $\varepsilon_U\{t,\sigma_U,T\}$. For example, one can choose the initial time $t=t_0$, temperature $T=T_0$, and applied stress $\sigma_U = \sigma_{U0}$ such that the corresponding strain is purely elastic and is given by:

$$\varepsilon_U\big|_{t=t_0} = \frac{\sigma_U}{E_U\big|_{T=T_0}} \qquad (12)$$

Except for some special cases, the above initial value problem requires a numerical solution method. One case amenable to exact solution is when the composite is subjected to a constant applied load at constant temperature $T=T_r$, and the fiber material undergoes inelastic (creep) in uniaxial tension according to the following relation:

$$\dot{\varepsilon}_f^i = A\sigma_f^n \qquad (13)$$

Then, $\lambda_{Uf} = \frac{3}{2}A\sigma_{Uf}^{n-1}$ and, for the initial condition given by Eq. (12), the solution is:

$$\varepsilon_U = \frac{V_f}{C_1 V_m E_m}\left[C_1\left(\frac{\sigma_U}{V_f} + R_f\right) - \left(C_2 + C_1\frac{(n-1)V_m E_m}{V_f}t\right)^{-1/n}\right], \qquad (14)$$

where, $C_1 = \left(AC_f\right)^{1/n}$ and $C_2 = \left[C_1\left(\frac{\sigma_U(1-C_m)}{V_f} + R_f\right)\right]^{1-n}$

Composite With Fully Cracked Matrix

Let us now consider a unit cell of length *2L*, width W_B, and uniform thickness *d*, of a composite in which all matrix has cracked. The field quantities specific to this damaged

composite are identified with the subscript "*B*". The composite is subjected to loading similar to that considered previously for undamaged composite.

It is assumed that once a crack in the matrix nucleates, it rapidly propagates, in directions normal to the load direction, to cover the entire width and depth of the matrix, arresting at or near the fiber-matrix interface, and causing a split of length *a* along the load direction (Figure 2). In line with the split, there is a distance *s* over which shear stress in non-zero. The effective Young's Modulus (E_{B2}) of region *B2* of length $(a+s)$ is $V_f E_f$.

Strain-rate of *Type B* cell can be expressed as:

$$\dot{\varepsilon}_B = \rho\dot{\varepsilon}_{B2} + (1-\rho)\dot{\varepsilon}_{B1} + \dot{\rho}\left(\varepsilon_{B2} - \varepsilon_{B1}\right) \tag{15}$$

in which, $\rho = (a+s)/L$. If the matrix is brittle or if there fibers within a tow are weakly bonded, *s* is expected to be much smaller than *a*. For the present, let us assume that this is the case and, therefore, $\rho \approx a/L$.

Note that region *B1* is structurally the same as the undamaged composite *(U)* considered previously. Therefore, strain rate $(\dot{\varepsilon}_{B1})$ of this region is given by Eq.(11) with the subscript "*U*" is replaced by "*B1*", and assigning $\sigma_{B1} = \sigma_B$.

$$\dot{\varepsilon}_{B1} = \left[\frac{\sigma_B - \left[E_m\left(\varepsilon_{B1} - \alpha_m(T - T_r)\right) + R_m\right]V_m}{V_f}\right]\left[\frac{2}{3}C_f\lambda_{B1f} + C_T\right] + C_{fm} + C_m D_t\left(\frac{\sigma_B}{V_m E_m}\right) \tag{16}$$

Strain rate in region *B2* is simply the strain rate in fiber under stress equal to σ_B / Vf, i.e.,

$$\dot{\varepsilon}_{B2} = D_t\left(\frac{\sigma_B}{V_f E_f} + \alpha_f(T - T_r)\right) + \frac{2}{3}\lambda_{B2f}\frac{\sigma_B}{V_f} \tag{17}$$

Thus, an expression for $\dot{\varepsilon}_B$ is found by substituting Eq. (16) and Eq. (17) in Eq. (15). An expression for growth rate of non-dimensionalized split length, ρ, can be assigned based on a suitable criterion. Eq. (15), together with appropriate initial conditions, can be solved for $\varepsilon_B\{t, \sigma_B, T\}$.

Composite With Progressive Matrix Cracks

We now consider a composite strip of length *2L*, width *W*, and uniform thickness *d*, of which any cross-section normal to the load contains cells of equal width, some undamaged *(Type U)* and some damaged *(Type B)* as shown in Figure 3. Let the ratio of the number of *Type* B cells to the total number of cells be η. Let the strip be subjected to applied stress $\sigma = P/(Wd)$ such that $\varepsilon_U = \varepsilon_B$. Then, stress acting on region *B* is given by:

$$\sigma_B = [\sigma - (1-\eta)\sigma_U]/\eta \tag{18}$$

and

$$\dot{\sigma}_B = \left[\dot{\sigma} - (1-\eta)\dot{\sigma}_U - \dot{\eta}\left(\frac{\sigma - \sigma_U}{\eta}\right)\right]\Big/\eta \tag{19}$$

The total strain and rates of strain for regions *U*, *B* and the composite are the same, i.e.,

$$\varepsilon = \varepsilon_U = \varepsilon_B \tag{20}$$

$$\dot{\varepsilon} = \dot{\varepsilon}_U = \dot{\varepsilon}_B \tag{21}$$

Rearranging Eq. (11), and using Eqs. (20) and (21), we have,

$$\dot{\sigma}_U = \frac{V_m E_m}{C_m}\left[\dot{\varepsilon} - \left[\frac{\sigma_U - [E_m(\varepsilon - \alpha_m(T - T_r)) + R_m]V_m}{V_f}\right]\left[\frac{2}{3}C_f\lambda_{Uf} + C_T\right] - C_{fm} - C_m\sigma_U D_t\left(\frac{1}{V_m E_m}\right)\right] \tag{22}$$

Substituting Eq. (22) in Eq. (19), we get,

$$\dot{\sigma}_B = \left[\dot{\sigma} - \frac{(1-\eta)V_m E_m}{C_m}\left[\dot{\varepsilon} - \left[\frac{\sigma_U - [E_m(\varepsilon - \alpha_m(T - T_r)) + R_m]V_m}{V_f}\right]\left[\frac{2}{3}C_f\lambda_{Uf} + C_T\right] - C_{fm} - C_m\sigma_U D_t\left(\frac{1}{V_m E_m}\right)\right]\right.$$
$$\left. - \dot{\eta}\left(\frac{\sigma - \sigma_U}{\eta}\right)\right]/\eta \tag{23}$$

Substituting Eqs. (19) and (23) in Eqs. (16) and (17), we get expressions for $\dot{\varepsilon}_{B1}$ and $\dot{\varepsilon}_{B2}$. These expressions, when substituted in Eq. (15), together with Eq. (20), provide the following expression for strain rate in composite with progressive matrix cracks:

$$\dot{\varepsilon} = \rho\dot{\varepsilon}_{B2} + (1-\rho)\dot{\varepsilon}_{B1} + \dot{\rho}(\varepsilon_{B2} - \varepsilon_{B1}) \tag{24}$$

The expression for $\dot{\varepsilon}$ includes integrated values σ, T, σ_U, ε_U^i, ε_{B1}^i and ε_{B2}^i. Therefore, the solution of Eq. (24) requires prescription of appropriate initial conditions for these variables. Additionally, expressions for $\dot{\rho}$ and $\dot{\eta}$, and corresponding initial conditions for ρ and η are needed.

Choice of ρ and η Functions

At a given load, the damage parameter η represents the fraction of the total number of matrix regions between fibers, normal to the load direction, that have cracks. Thus, using Weibull statistics, we choose the following function for η:

$$\eta = \eta_0 + (1-\eta_0)\left[1 - e^{-0.693\left(\frac{\sigma_m}{\sigma_0}\right)^{\eta_N}}\right] \quad \text{for } \sigma_m \geq 0 \qquad (25)$$

$$= 0 \qquad \text{for } \sigma_m < 0$$

In the above, σ_m is the maximum of the stress in the matrix in regions *U* and *B1*, η_N is the Weibull modulus, η_0 is initial value of η and σ_0 is median strength of the matrix. At $\sigma_m = \sigma_0$, η=*0.5*. Both η_N and σ_0 may be temperature and time dependent. For example, σ_0 may decrease with time due to the environment-induced degradation of the matrix, or with number of load cycles due to fatigue.

An expression for the second damage parameter ρ should be based on fracture mechanics concepts. In so far as the split is induced by the arrest of a transverse crack in the matrix, it can be argued that its initial length is proportional to the stress intensity factors associated with the matrix crack. Assuming that, on the average, each matrix crack is of equal length – say, the average fiber spacing, then the associated stress intensity factors are linear functions of only σ_m. Thus, it can be argued that the initial split length is a function of only σ_m. However, subsequent growth of the split would be dictated by the stress intensity factors associated with the tip of the split itself.

Even if it is possible to estimate stress intensity factors associated with a growing split, eventually an empirical approach would be needed to develop growth rate criteria for the splits, requiring measurements of split length as it would grow under load. At present, such measurements are infeasible even under ambient conditions. What may be feasible is to infer split growth rate criteria from global deformation characteristics of the composite.

Considering the above difficulties, let us consider an opportunistic approach and assume that the functional form of ρ is the same as of η. Specifically, we assume that:

$$\rho = \rho_0 + (1-\rho_0)\left[1 - e^{-\rho_c\left(\frac{\sigma_m}{\sigma_0}\right)^{\rho_N}}\right] \quad \text{for } \eta \geq 0 \qquad (26)$$

$$= 0 \qquad \text{for } \eta < 0$$

In the above, ρ_C and ρ_N are time and temperature dependent parameters and ρ_0 is initial value of ρ. It is shown later that the above choice of ρ allows modeling of a broad spectrum of global deformation characteristics of composites. By interpreting the η and ρ parameters as measures of the matrix cracks parallel to and perpendicular to the fibers respectively, the product of η and ρ can be interpreted as "crack density" in a two-dimensional sense.

In summary, the determination of damage state, defined by ρ and η, requires inferring the values of σ_0, η_N, ρ_C and ρ_N for the composite. In principle it should be possible to find σ_0 and η_N using statistical distribution of strength of the matrix; at least in cases, such as some unidirectional composites, where matrix represents a single monolithic material. However, in general, this is not feasible. Instead, like ρ_C and ρ_N, σ_0 and η_N must be inferred using a composite's global deformation characteristics.

Progressive Failure of the Fibers

As will be shown later the effect of matrix cracking as modeled by the η and ρ functions of equations (25) and (26) is to reduce the modulus of the composite and thus introduce nonlinearity in the composite stress-strain behavior. As more of the matrix cracks the composite strain increases until finally the fiber strain approaches its critical value at failure. The failure of the reinforcements in turn leads to the ultimate failure of the composite. Thus in theory it should be possible to model the final failure of the composite using the failure statistics of *in-situ* fibers. Using a Weibull form to model the failure of the *in-situ* fibers we can write the following expression for the fraction of unbroken fibers:

$$\psi = exp\left\{\psi_c\left(\frac{\varepsilon-\varepsilon_0}{\varepsilon_f-\varepsilon_0}\right)^{\psi_n}\right\} \qquad \text{for } \varepsilon \geq \varepsilon_0 \tag{27}$$

where ε_0 is the minimum value of strain where the fiber starts to fail and ψ_c and ψ_n are parameters defining the Weibull distribution. As before by setting $\psi_c = -0.693$, ε_f becomes the median failure strain of the *in-situ* fibers. In the absence of fiber failure strain data we can estimate the remaining Weibull parameters in equation 27 from the composite failure data. The ψ parameter is then used to progressively reduce the volume fraction of the fibers in the composite.

Solution of the CMC Model

Exact solution of the CMC model described by equation (24) can be obtained for the special case of a two-phase composite in which the fiber and the matrix materials are both linear elastic. For this case non-linear stress-strain behavior of the damaged composite can be described by the relation

$$\sigma = \overline{E}\varepsilon \tag{28}$$

where $\overline{E}$ is the effective modulus of the composite containing matrix cracks and is given by

$$\overline{E} = (1-\eta)E_c + \eta\left[\frac{V_f E_f E_c}{(1-\rho)V_f E_f + \rho E_c}\right] \tag{29}$$

Here E_c is the modulus of the undamaged composite, which is also the modulus of cell-U, given by equation (8). Equation (28) can be evaluated in closed-form after substituting the expressions (25) and (26) for the η and ρ functions respectively and by noting that the matrix stress in these expressions is simply

$$\sigma_m = E_m(\varepsilon - \alpha_m(T - T_r)) + R_m \tag{30}$$

where E_m, α_m and R_m are respectively the Young's modulus, CTE and the residual stress of the effective matrix.

A more general application of the foregoing model requires numerical solution of the equation (24) together with appropriate initial conditions. In the present work the numerical solution method used is the fourth-order Runge-Kutta method [18].

Figure 4(a) shows the stress-strain response of a CMC determined using the finite-difference numerical solution method. The solution, obtained using two different values of time-step, Δt, is compared with the exact solution determined using equation (3.34). The values of the material constants and damage parameters used to determine the solution are also included in the figure. The results indicate that as the time step is decreased the numerical solution converges to the closed-form solution. Similar comparison of the damage functions, η and ρ, obtained using the two solution techniques are shown in Figure 4(b). The results demonstrate the accuracy of the finite-difference numerical solution method used to solve the nonlinear equations.

Results and Discussion

Figures 5, 6 and 7 show the room-temperature (RT) tensile stress-strain curves of three ceramic-matrix composites generated using the present model and the corresponding laboratory test measurements. Note that the numerical solutions are not predictions. Rather, with the exception of fiber properties and architecture specifics of the composite, all other input data for the model were found using the measurements shown in the figures. While the solutions are not direct curve-fits of the measured data, they are nevertheless "calibrations" needed to establish the various composite specific properties and damage parameters shown in Table 1. The effect of the coating in coated fibers is included in the transverse modulus of the fiber listed in the table. The table also lists the references in which the test data analyzed in this work have been reported.

Note that a single tensile test is needed to determine values of all needed constants relevant to the laboratory test conditions. Furthermore, the model is versatile enough to capture the significantly different deformation characteristic of the composites with sufficient accuracy. While the tensile stress-strain curve of the two cross-ply Sylramic^{TM}-iBN/SiC (silicon carbide) composites shown in Figure-5 have a bilinear

profile, the cross-ply Nicalon^{TM}/SiC composite shown in Figure-6 shows nonlinear behavior early during load-up. The tensile response of the latter lacks a distinct 'knee' in the curve. Figure-7 shows a second stiffening in the tensile behavior of unidirectional Nicalon^{TM}/CAS (calcium alumino-silicate) composite close to failure. The model does capture this behavior, but has to include fiber failure to accurately model the observed data. In all cases it was found that the median strength of the matrix, σ_0, approximately coincided with the stress in the matrix in undamaged composite corresponding to the proportional limit in the stress-strain curve of the composite.

Figure 8 shows the predicted stress-strain behavior of a SiC/SiC composite when it is unloaded from certain load levels, and re-loaded. Upon unloading the composite is predicted to have linear stress-strain response such that there is full recovery of the strain when the composite is fully unloaded. This is consistent with the assumption that the nonlinearity observed during tensile loading is primarily due to micromechanical damage of the matrix. The prediction using the above model required no additional calibration beyond that described earlier. As shown, the prediction is in general agreement with measurements. Unloading portions of the data indicate damage accumulation with increasing load. Similar prediction of the change in the secant modulus of unidirectional SiC/glass composite is shown in Figure 9. Again there is good agreement between the data and the model prediction.

Figure 10(a) shows damage state at room temperature, represented by the parameters η and ρ, plotted against increasing applied tension, for the SiC/SiC composite 009 shown in Figure 5. The product of the two damage parameters is also plotted in the figure. This quantity, which is the product of the transverse and longitudinal normalized total crack lengths, can be interpreted as a measure of the crack density in the matrix. The plot shows that below a critical value of the applied stress there are no significant cracks in the matrix. Matrix cracking starts as soon as the compressive matrix stress in the matrix is overcome by the applied stress. The value of the applied stress when this occurs is the critical 'matrix cracking stress' in Figure 10(a). Beyond this value of the load the micro damage in the matrix progressively increases until it approaches saturation. It can also be observed in Figure 10(a) that the η parameter becomes 0.5 at applied stress of 166 MPa, which is close to the proportional limit of the 009 composite in Figure 5. Thus according to the CMC model presented here the density of the transverse cracks approaches half its value at saturation near the proportional limit of the composite.

The product of the damage parameters η and ρ is plotted against the applied stress in Figure 10(b) for the two different SiC/SiC composites shown in Figure 5. This quantity, which is the product of the transverse and longitudinal normalized total crack lengths, can be interpreted as a measure of the crack density in the matrix. The plot also shows the linear crack density estimated from the acoustic energy (AE) response of the two composites as reported in reference [19]. AE is a measure of the acoustic signals associated with matrix cracking and so the AE curve is a measure of the number of matrix cracks in the composite. Thus even though there is no one-to-one correlation between the quantity $\rho^*\eta$ and the AE curve they can be compared in a qualitative sense

since they both are measures of the growth of matrix cracks in the composite. Figure 10(b) shows that the AE curve and the product of η and ρ both have a sigmoidal profile: they both start slowly and increase rapidly before approaching a saturation value. In the CMC model cracking starts only after the matrix residual stress is overcome. Since the damage functions ρ and η of the above CMC model are normalized their product approaches a value of 1.0 that corresponds to fully cracked matrix. Another observation that can be made from Figure 10(b) is that the quantity $\rho^*\eta$ preserves the material ranking seen in the AE data. Thus the matrix in the 009 material is predicted by the model to crack more rapidly than that in the 011 material and this is consistent with the AE data.

The growth of the damage parameters η and ρ in the Nicalon^{TM}/SiC composite along with that of their product with the applied stress is shown in Figure 11. As shown in Figure 6 the stress-strain behavior of this composite exhibits nonlinear behavior at a very small load. The damage functions in Figure 11 shows that the damage growth starts at a much lower value of the applied stress as compared to the SiC/SiC composites in Figure 10.

Crack density in SiC/glass determined by counting the individual cracks in the specimen gage area are reported in reference [1]. Figure 12 compares the damage state prediction using the present model, represented by the product of η and ρ, with the crack density data for this material. In this case too the model captures the matrix crack growth behavior observed in the data.

As mentioned earlier with the exception of fiber properties and architecture specifics of the composite, all other input data for the model were found from the stress-strain data. Due to the highly nonlinear nature of the problem it is difficult to obtain a rigorous mathematical proof of the uniqueness of the damage constants for each composite. However we can use the closed-form expression (28) determine an optimized set of damage constants that best agree with the test data. All the damage constants reported in this work were determined in this manner.

The advantage of this model is that once the CMC material is characterized the model can be used to study the effect of varying geometry and loads. Further since the model is described in terms of the basic constituent properties it can also be used to estimate the effect of changing variables such as porosity and fiber volume fraction. The predicted tensile response of Sylramic^{TM}-iBN/SiC CMCs with different volume fractions is compared with test data from reference [19] in Figure 13. The model predictions were all made using the constituent properties determined from the 011-CMC data (Table-1). The CMCs in Figure 13 seem to differ in more than just their volume fraction as indicated by their initial modulus not changing monotonically with the fiber content. The model does however capture the ranking and profile of the overall behavior of the composites. This application of the above CMC model illustrates how it can be used in material evaluation.

Another feature of the model is the coupling of the constituent material inelasticity with damage. As an example we use the equations to model the time-dependent behavior of oxide/oxide composites in which the matrix cracks easily while the fiber creeps under

load. Figure 14 shows the comparison of the solution from the model with test data [21] from woven cross-ply composite with Nextel™720 fiber and alumina-silicate (AS-0) matrix. To capture the observed composite behavior we assume the fiber strain rate, $\dot{\varepsilon}_f^i$, to follow the relation

$$\dot{\varepsilon}_f^I = 1.6x10^{-12}\sigma_f^{2.73}t^{-0.755} \tag{31}$$

Here the fiber stress, σ_f, is expressed in MPa and time, *t*, is in seconds. The other material properties, including damage constants, used to do the modeling are given in Figure 14. Thus as the fiber creeps and the matrix cracks they shed load to each other so that both, the amount of creep and the crack density, increase continuously with time; though in this example the increase in damage strain is not significant. Figure 15 shows the predicted change in the creep and damage strains up to 3 hours when the matrix becomes fully cracked and the damage strain reaches a steady state value.

Conclusion

In this paper we present a mechanics based life-prediction model for brittle matrix composites that considers the deformation due to dominant damage mechanisms such as matrix microcracking and fiber-matrix debonding. The model also includes consideration of inelastic deformation of one of the constituents such as creep of the fiber. All the material properties and model constants can be obtained by charactering a single tension and single creep test of the material under each test condition. Once characterized the model can be used to predict the behavior under other geometry and load conditions. The model also determines the damage state of the material under load. Examples of the application of the model to several ceramic matrix composites with similar damage mechanisms have been presented. This modeling approach can be used in as a basis to develop a comprehensive life prediction model.

Acknowledgement

Part of this work was supported by the United States Air Force under Contract No. FA8650-03-C-5228.

References

1. Karandikar, P. G., and Tsu-Wei Chou, “Characterization and Modeling of Microcracking and Elastic Moduli Changes in Nicalon-CAS Composites”, Composites Science and Technology, 46 (1993) 253-263.
2. Zhu, S., Mizuno, M., Kagawa, Y. and Mutoh, Y. , “Monotonic Tension, Fatigue and Creep Behavior of SiC Fiber reinforced SiC-Matrix Composites: A Review”, Composites Science and Technology, 59, pp. 833-851, 1999
3. DiCarlo, J. A., Yun, H. M., and Hurst, J. B., “Fracture Mechanisms for SiC Fibers and SiC/SiC Composites under Stress-Rupture Conditions at High Temperatures”, Applied Mathematics and Computation, 152 (2004) 473–481.

4. Morscher, G. N., and Cawley, J. D., "Intermediate Temperature Strength Degradation in SiC/SiC Composites", Journal of the European Ceramic Society, 22 (2002) 2777–2787.
5. Eckel, A. J., Cawley, J. D. and Parthasarathy, T., "Oxidation of a Continuous Carbon Phase in a Nonreactive Matrix", J. Am. Ceram. Soc., 78 (1995) 972–980.
6. Aveston, J, Cooper, G.A., and Kelly, A., "Single and Multiple Fracture", The Properties of Fiber Composites, IPC Science and Technology Press, Ltd, pp, 15-24, 1971
7. Marshall, D.B., Cox, B.N. and Evans, A.G., The mechanics of matrix cracking in brittle matrix composites, Acta Metal., 1986, Vol 33, pp2013-2021
8. Curtin, W.A., Ahn, B.K., and Takeda, N., Modeling brittle and tough stress-strain behavior in unidirectional ceramic matrix composites, Acta Metal., 1998, Vol 46, pp3409-3420.
9. Budiansky, B., Hutchinson, J. W. and Evans, A. G., "Matrix Fracture in Fiber Reinforced Ceramics", *J. Mech. Phys. Solids*, 34 (1986) 167-189.
10. Begley, M.R., Evans, A.G. and McMeeking, R.M., "Creep Rupture in Ceramic Matrix Composites with Creeping Fibers", J. Mech Phys. Solids, 1995, Vol 43, pp727-40.
11. Genin, G. M. and Hutchinson, J. W., "Composite Laminates in Plane Stress: Constitutive Modeling and Stress Redistribution due to Matrix Cracking", J. American Ceramic Society, Volume 80 Issue 5, Pages 1245 – 1255.
12. Yen, C-F and Jones, M. L., "Material Modeling for Cross-Ply Ceramic Matrix Laminates with Progressive Damages and Environmental Degradation", in MD-Vol. 80, Composites and Functionally Graded Materials, ASME 1997, 189-2002.
13. Okabe, T., Komotori, J. and Shimizu, M., "Mechanical Behavior of SiC Fiber Reinforced Brittle Matrix Composites", J. Materials Science, 34 (1999), 3405-3412.
14. Vanswijgenhoven, E., Wevers, M. and Biest, O. V. D., "The Transverse Strain Response of Cross-Plied Fiber-Reinforced Ceramic-Matrix Composites", Composites Science and Technology, 59 (1999), 1469-1481.
15. Camus, G., "Modeling of the Mechanical Behavior and Damage Process of Fibrous Ceramic Matrix Composites: Application to a 2D SiC/SiC", Int. J. Solids and Structures, 37 (2000) 919-942.
16. Jones, R. M., Mechanics of Composites Materials, 2d. Ed., Taylor and Francis, Inc., Philadelphia, PA, 1999.
17. Gatewood, B. E., Thermal Stresses, McGraw-Hill Book Co., New York, 1957.
18. Ferziger, J. H., Numerical Methods for Engineering Applications, John Wiley & Sons, New York, 1981.
19. Morscher, G. N., "Stress-dependent matrix cracking in 2D woven SiC-fiber reinforced melt-infiltrated SiC matrix composites", Composites Science and Technology 64 (2004) 1311–1319.
20. Pluvinage, P., Parvizi-Majidi, A., and Chou, T.W., "High Temperature Behavior of 2D-Woven and 3D Braided SiC/SiC Composites," High Temperature Ceramic Matrix Composites; Proceedings of the 6th European Conference on Composite Materials, eds. R. Naslain, J. Lamon, and D. Doumeingts (United Kingdom: Woodhead Publishing, Ltd., 1993), 675-682.

21. John, R., Buchanan, D. J., and Zawada, L. P., "Fracture and Creep Rupture Behavior of Notched Oxide/Oxide and SiC/SiC CMC", Proceedings, 10th International Congress of Fracture (ICF10), Honolulu, Hawaii, 3-7 December 2001.

APPENDIX

The properties of the effective matrix (*m*), which includes the actual matrix (*M*) and the transverse fibers in a balanced cross-ply composite, are given by

$$E_m = \frac{\lfloor E_1 - E_f \nu_f / 2 \rfloor}{1 - \nu_f / 2} \tag{A1}$$

$$\alpha_m = \frac{\alpha_1 \lfloor E_f \nu_f / 2 + E_m (1 - \nu_f / 2) \rfloor - E_f \alpha_f \nu_f / 2}{E_m (1 - \nu_f / 2)} \tag{A2}$$

where the effective properties of the cross-ply composite along a fiber direction are given by

$$E_1 = \frac{E_L + E_T}{2} \tag{A3}$$

$$\alpha_1 = \frac{E_L \alpha_L + E_T \alpha_T}{2 E_1} \tag{A4}$$

and the longitudinal (L) and transverse (T) properties of a single ply are given by

$$E_L = E_f \nu_f + E_M (1 - \nu_f) \tag{A5}$$

$$E_T = \frac{E_{fT} E_M}{\left[E_M \nu_f + E_{fT} (1 - \nu_f) \right]} \tag{A6}$$

$$\alpha_L = \frac{E_f \alpha_f \nu_f + E_M \alpha_M (1 - \nu_f)}{E_L} \tag{A7}$$

$$\alpha_T = (1 + \nu_f) \alpha_f \nu_f + (1 + \nu_M) \alpha_M (1 - \nu_f) - \alpha_L \lfloor \nu_f \nu_f + \nu_M (1 - \nu_f) \rfloor \tag{A8}$$

Table-1: Properties of CMCs

CMC	1 [1]	120 [20]	009 [19]	011 [19]	068 [19]
Geometry	Unidirectional	0/90 PW[1]	0/90 5H-SW[2]	0/90 5H-SW[2]	0/90 5H-SW[2]
v_f	0.35	0.43	0.36	0.38	0.40
p	0.00	0.09	0.05	0.05	0.05
T_p (°C)	1000	1450	1450	1450	1450
Fiber	Nicalon™	Nicalon™	Sylramic™-BN	Sylramic™-BN	Sylramic™-BN
E_{fL} (GPa)	190	200	333	333	333
E_{fT} (GPa)	190	180	173	173	173
v_f	0.17	0.17	0.17	0.17	0.17
α_f (µ/°C)	3.55	3.90	2.70	2.70	2.70
Matrix	CAS	CVI-SiC	MI-SiC	MI-SiC	MI-SiC
E_m (GPa)	93	295	331	181	321
v_m	0.125	0.125	0.125	0.125	0.125
α_m (µ/°C)	4.75	3.50	2.10	2.10	2.10
σ_0 (MPa)	256	47	140	158	365
η_N	2.648	0.410	0.459	0.518	0.770
ρ_c	-0.119	-0.050	-0.117	-0.190	-1.674
ρ_N	3.945	1.200	1.602	1.746	2.867

1 PW - Plain Weave

2 5H-SW - 5 Harness Satin Weave

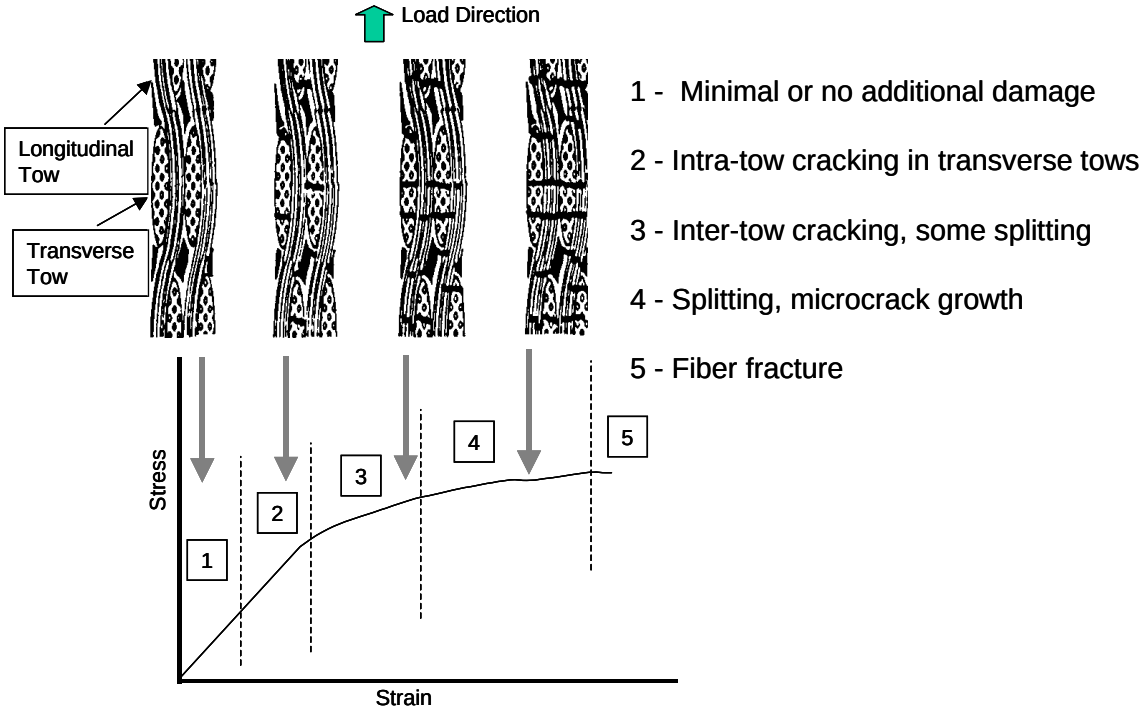

Figure 1(a): Response of SiC/SiC CMC under uniaxial tension.

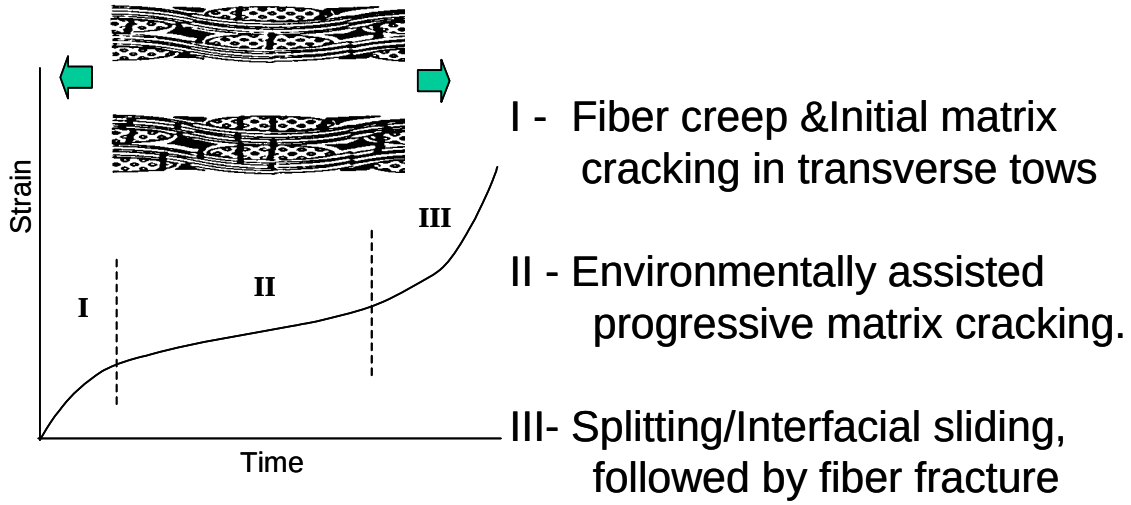

Figure 1(b): Response of SiC/SiC CMC under sustained loading.

Fiber Material:
Elastic/Inelastic

Matrix Material:
Elastic

***a*=Debond Length**
***s*=Shear Lag Length**

$$\rho = \frac{a+s}{l}$$

$$\eta = \frac{Number\ of\ Type\ B\ Cells}{Number\ of\ Type\ U\ Cells}$$

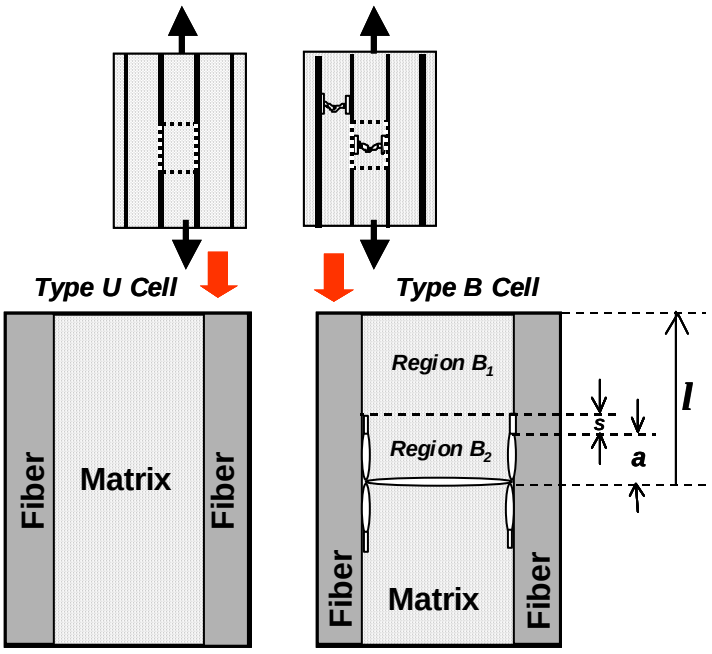

Figure 2: Unit Cells in CMC Damage Model.

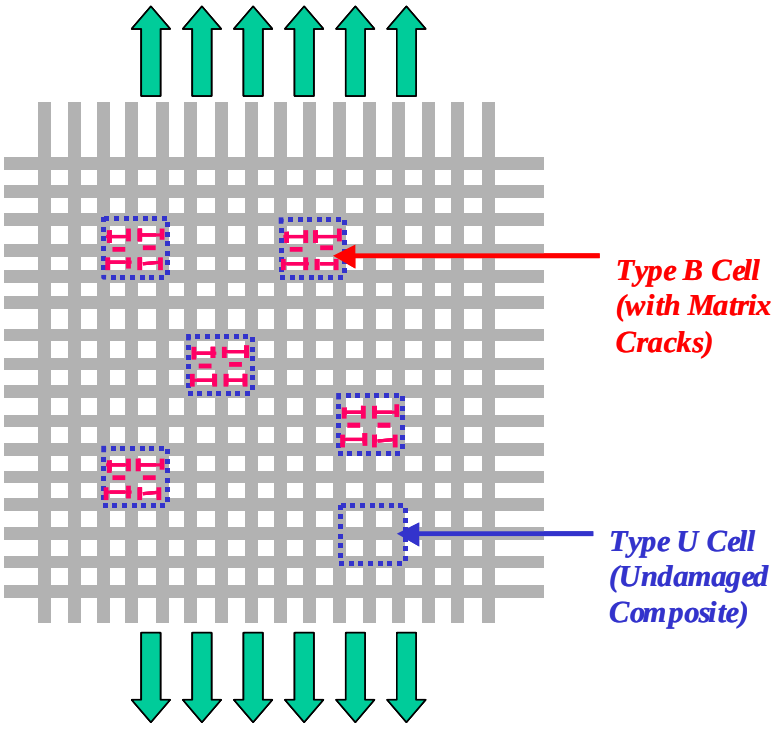

Figure 3: CMC Damage Model.

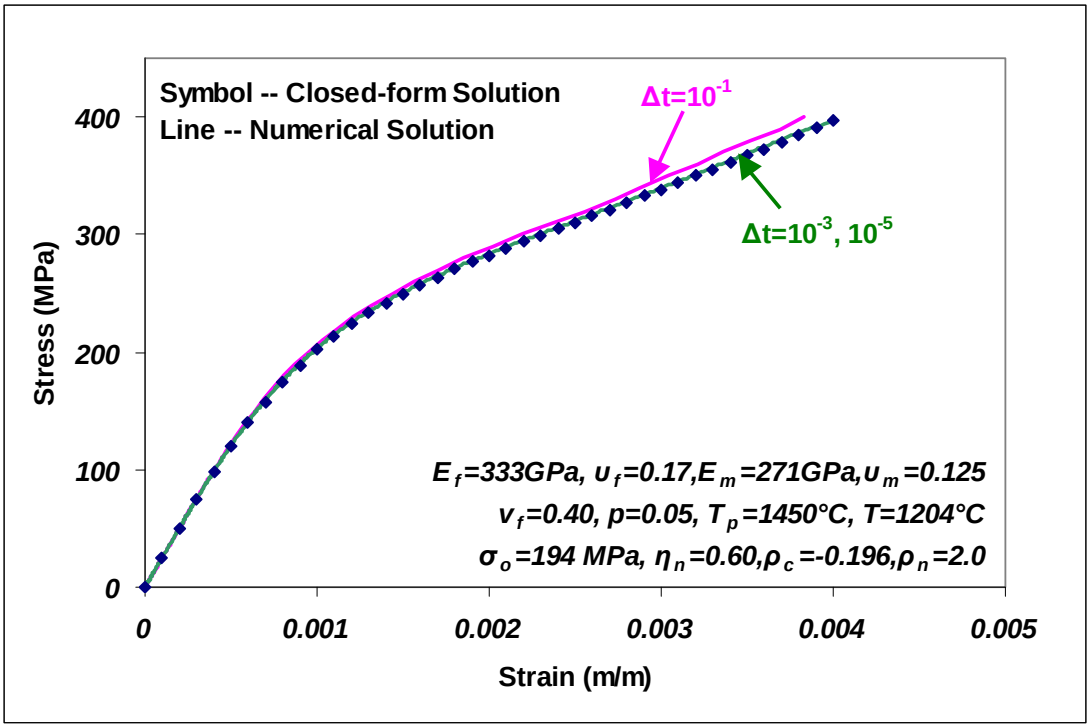

Figure 4(a): Comparison of Numerical Solution with Exact Solution of CMC Model.

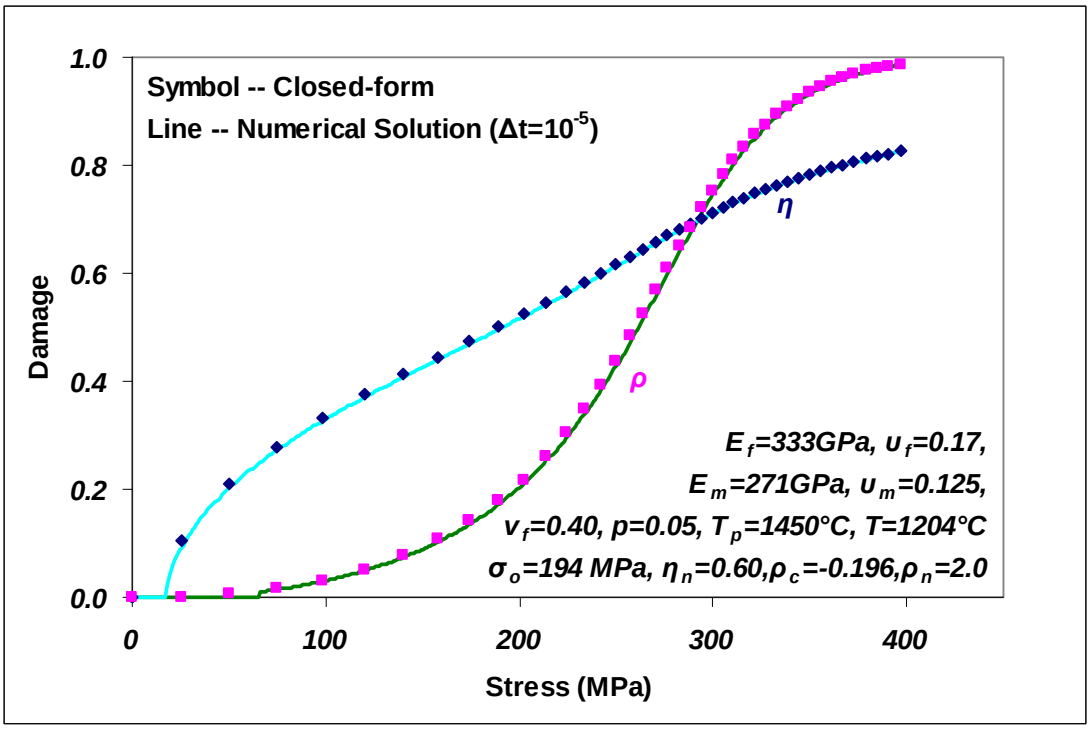

Figure 4(b): Evolution of Damage Functions in CMC Model.

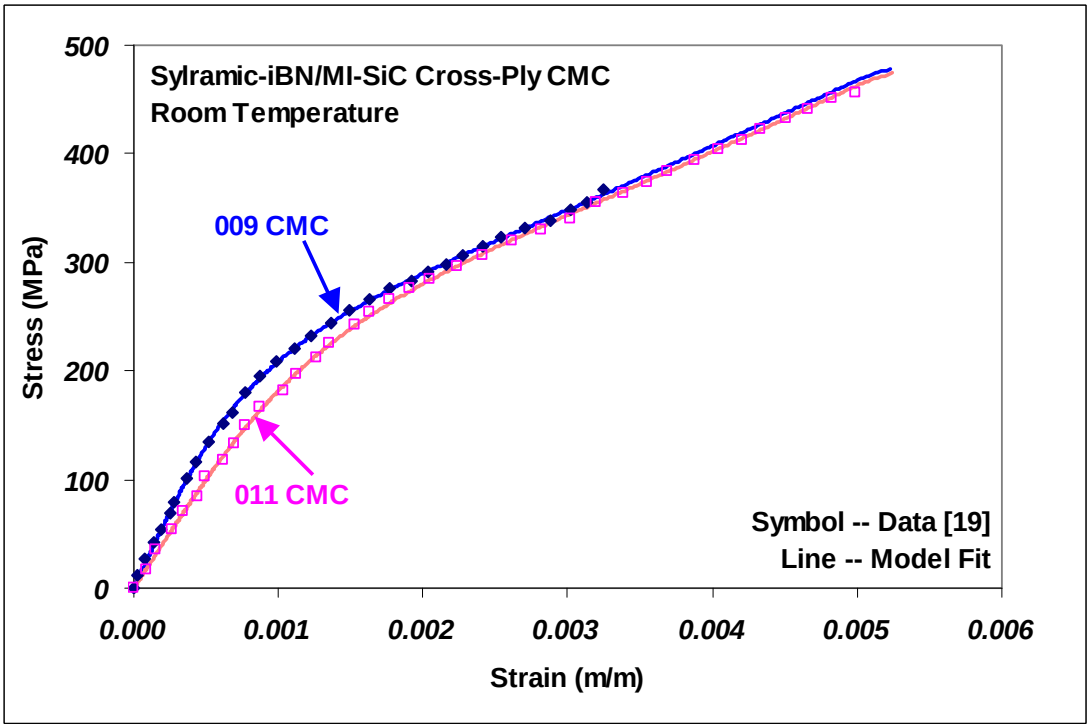

Figure 5: Tensile Response of Sylramic-iBN/MI-SiC Cross-Ply CMCs.

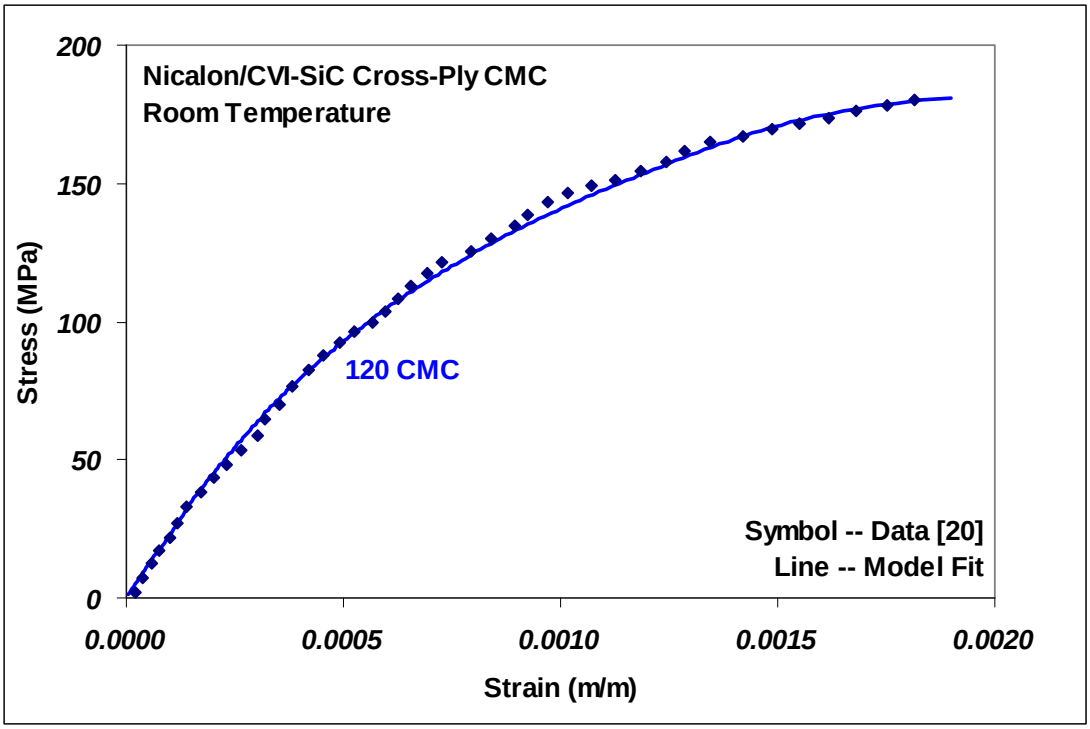

Figure 6: Tensile Response of Nicalon/CVI-SiC Cross-Ply CMC.

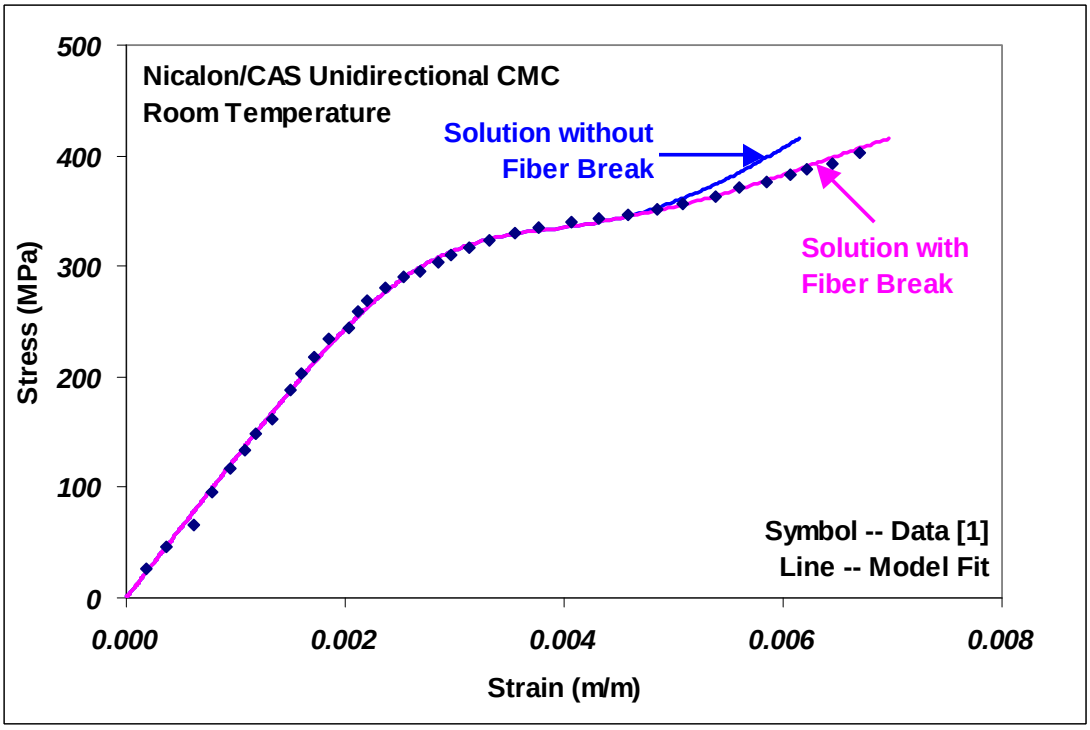

Figure 7: Tensile Response of Nicalon/CAS Unidirectional CMC.

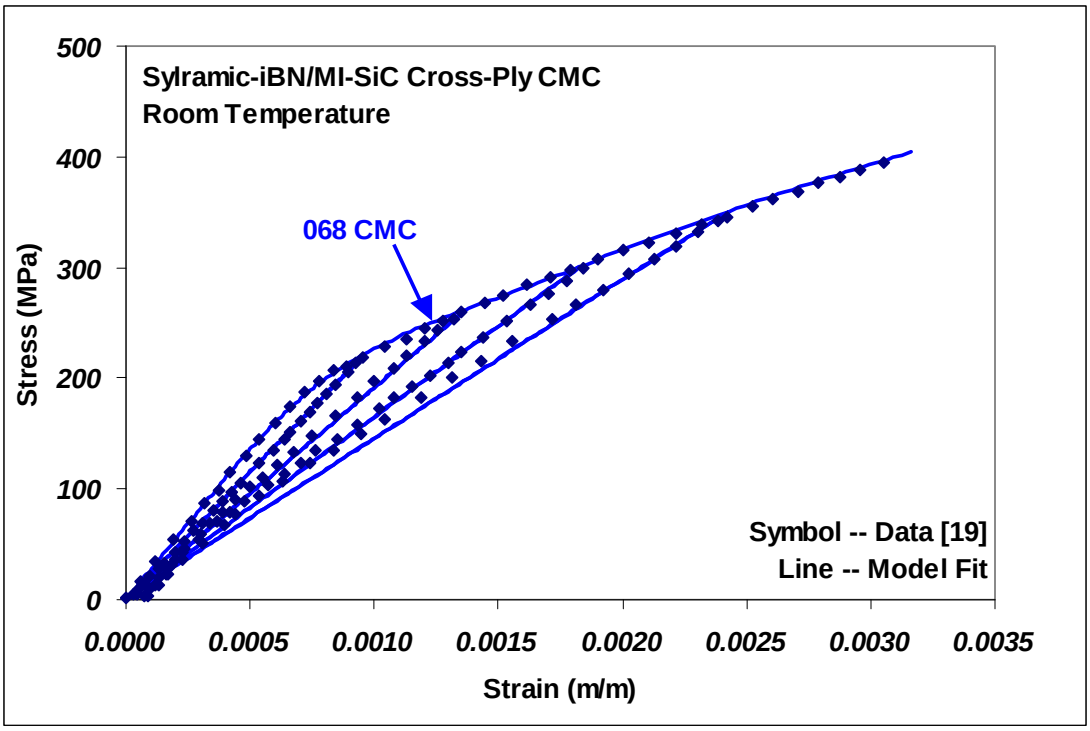

Figure 8: Tensile Load-Unload Response of Sylramic-iBN/MI-SiC Cross-Ply CMC.

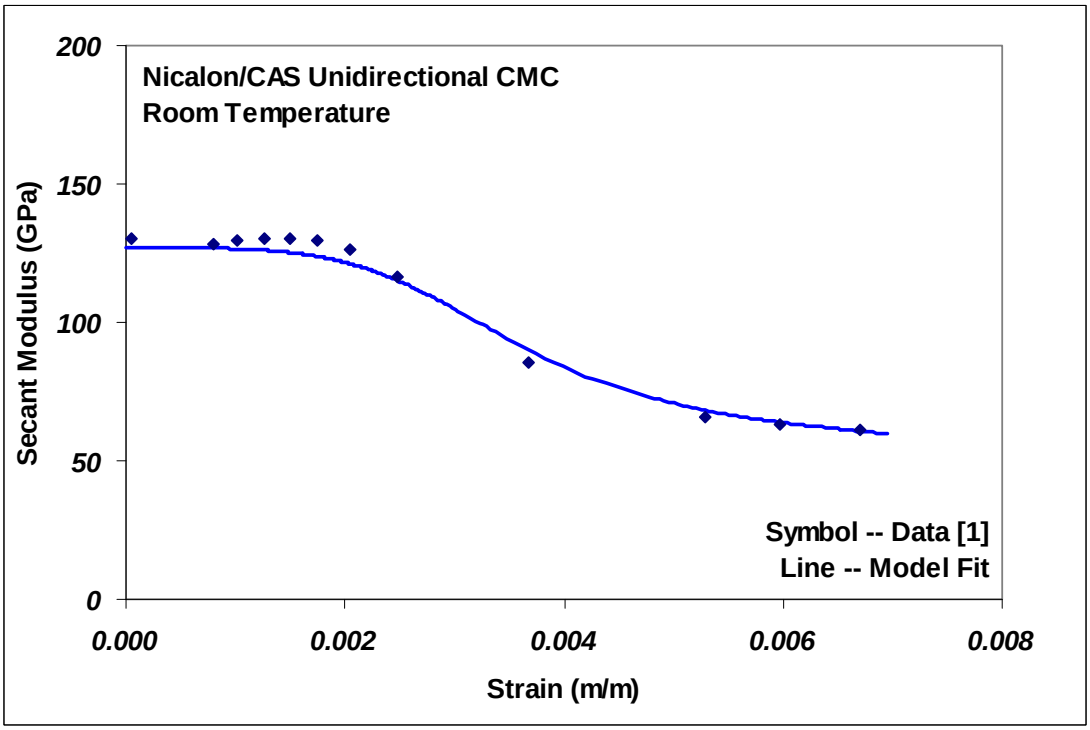

Figure 9: Change in Secant Modulus of Nicalon/CAS Unidirectional CMC.

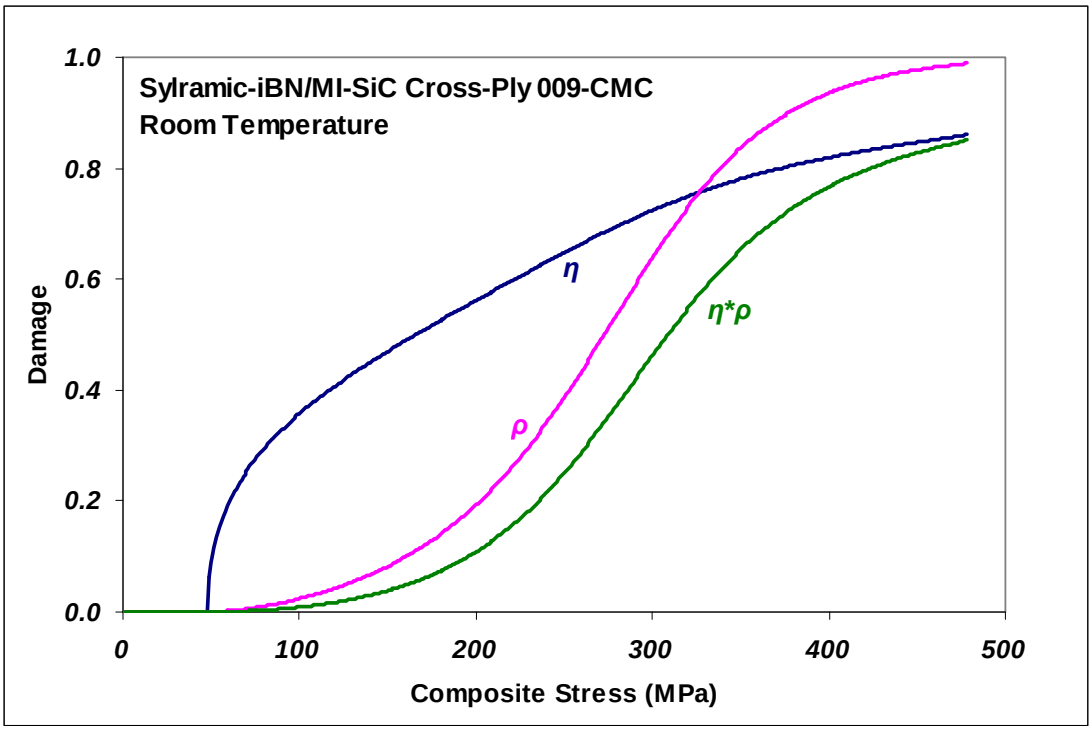

Figure 10(a): Damage Evolution in Sylramic-iBN/MI-SiC Cross-Ply CMC.

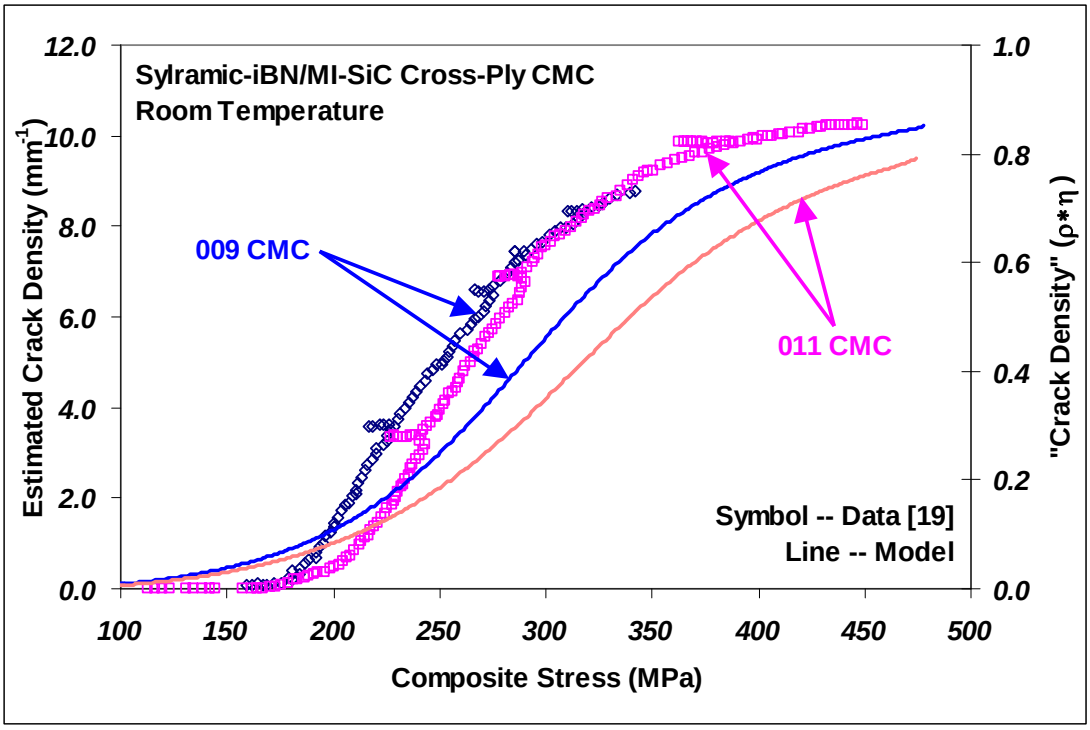

Figure 10(b): Comparison of Damage Evolution in Sylramic/MI-SiC Cross-Ply CMCs.

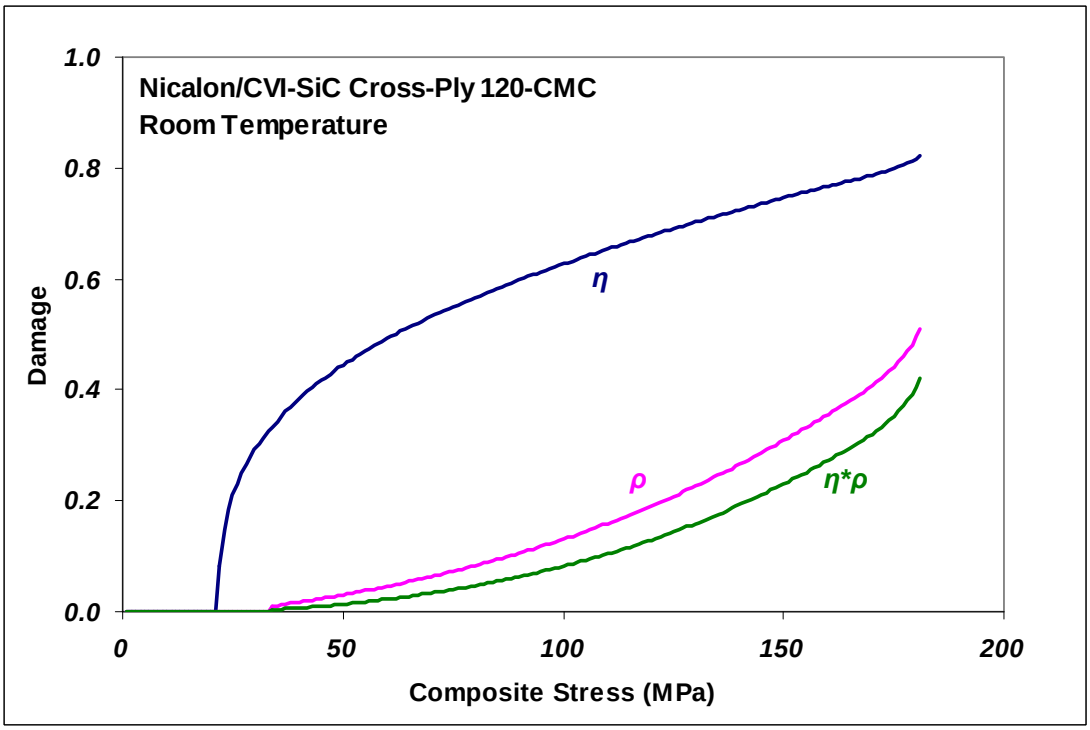

Figure 11: Damage Evolution in Nicalon/CVI-SiC Cross-Ply CMC.

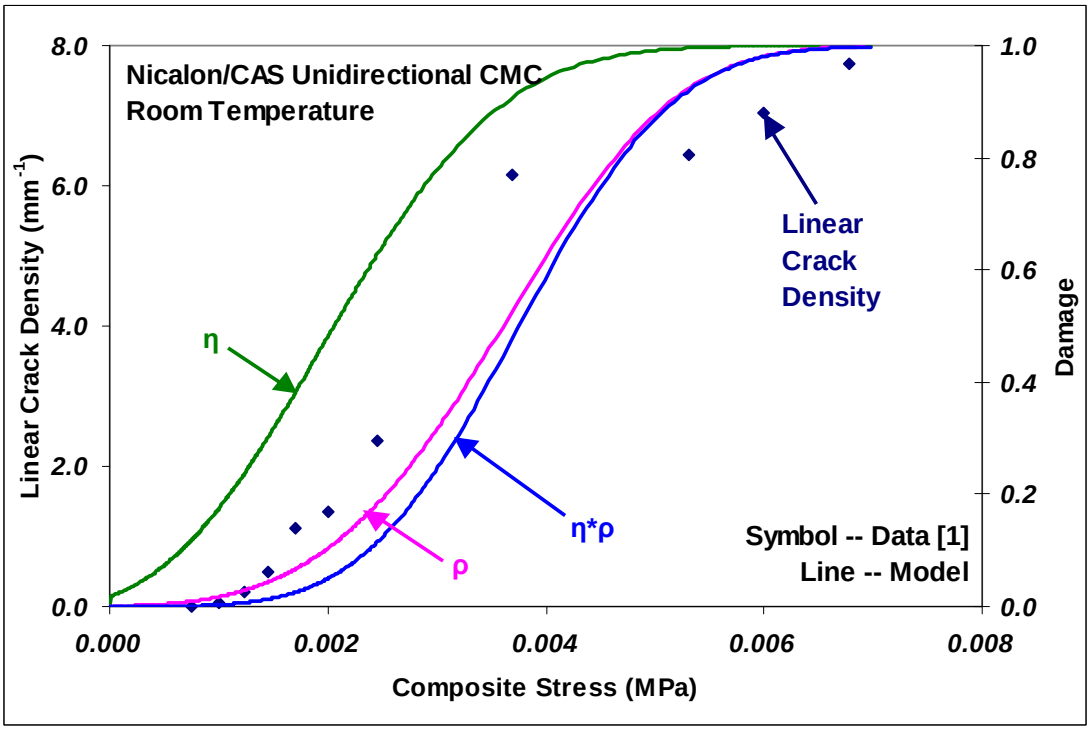

Figure 12: Damage Evolution in Nicalon/CAS Unidirectional CMC.

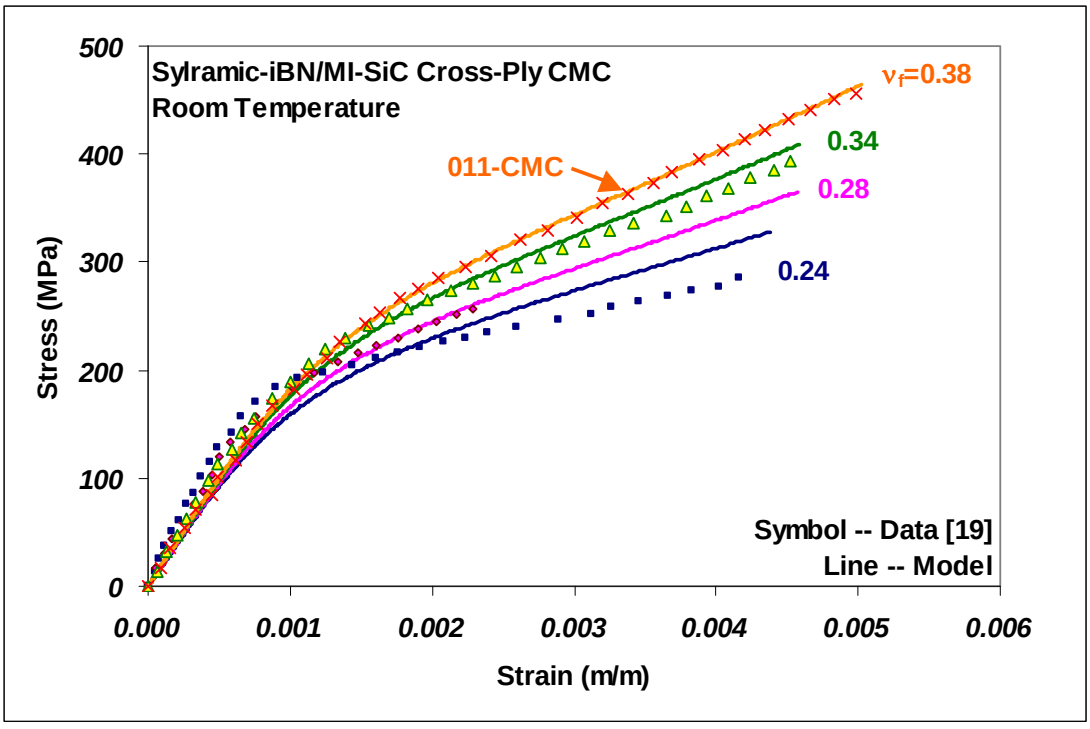

Figure 13: Effect of Volume Fraction on Sylramic-iBN/MI-SiC Cross-Ply CMC.

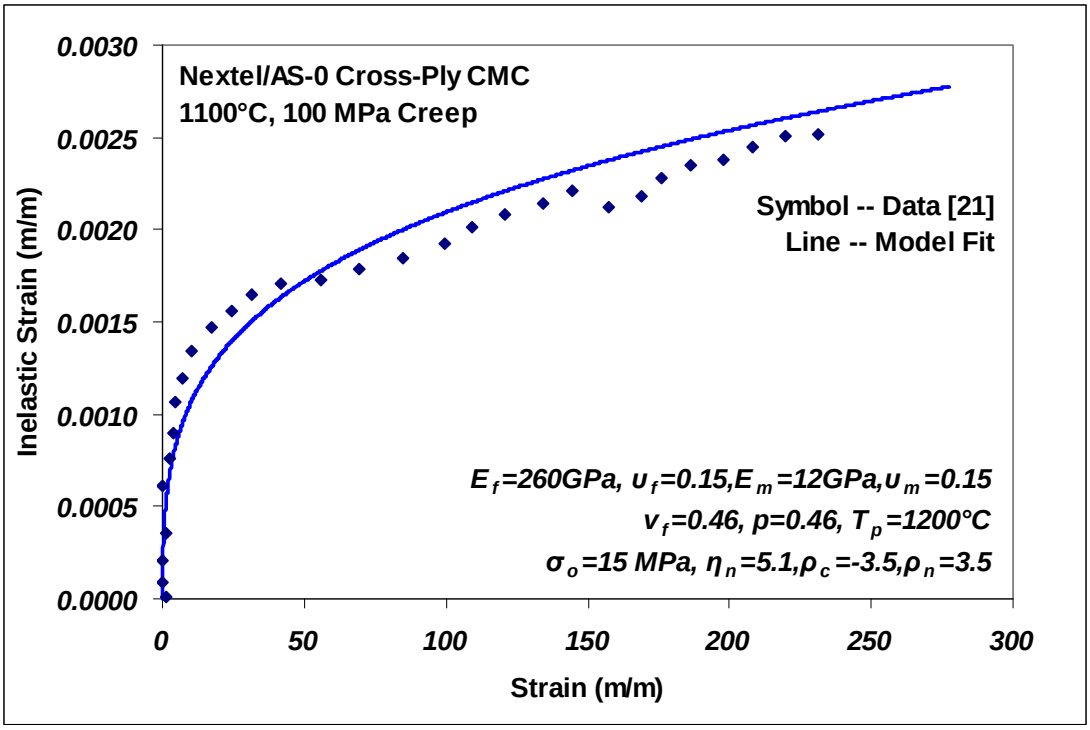

Figure 14: Creep Deformation in Nextel/AS-0 Cross-Ply CMC.

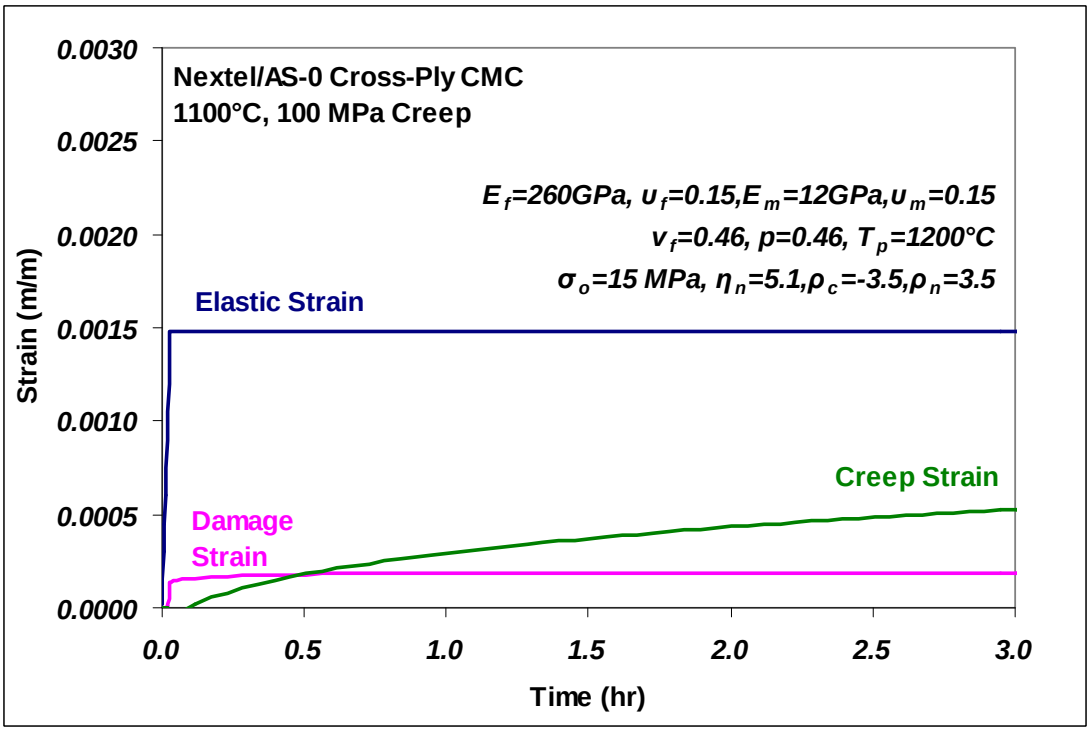

Figure 15: Change in Strain Components During Creep of Nextel/AS-0 Cross-Ply CMC.